A novel chaotic system and its topological horseshoe

Chunlai Li [a1], **Lei Wu** [b], **Hongmin Li** [c], **Yaonan Tong** [c]

[a]College of Physics and Electronics
Hunan Institute of Science and Technology
Yueyang 414006, China
hnistlichl@163.com

[b]Department No. 6 of Air Force Paratrooper College
Guilin 541003, China
5950595@qq.com

[c]College of Information and Communication Engineering
Hunan Institute of Science and Technology
Yueyang 414006, China
lihmin171@sina.com; pjtyn@163.com

Received: 10 February 2012 / **Revised:** 16 July 2012 / **Published online:** 25 January 2013

Abstract. Based on the construction pattern of Chen, Liu and Qi chaotic systems, a new three-dimensional (3D) chaotic system is proposed by developing Lorenz chaotic system. It's found that when parameter e varies, the Lyapunov exponent spectrum keeps invariable, and the signal amplitude can be controlled by adjusting e. Moreover, the horseshoe chaos in this system is investigated based on the topological horseshoe theory.

Keywords: chaotic system, invariable Lyapunov exponent spectrum, amplitude control, topological horseshoe.

1 Introduction

In 1963, Lorenz discovered a chaotic system when studying the atmospheric convection [1]. As the first chaotic model, Lorenz system has become a paradigm for chaos investigation [2–7]. Many three-dimensional chaotic systems have been proposed by developing Lorenz chaotic system, such as Chen system [4], Liu system [5], Qi system [6], Lü system [7]. Due to powerful applications in chemical reactions, cryptology, nonlinear circuits, secure communication and so on, researchers have paid great attention to generate new chaotic systems and analyse their dynamical behaviors and dynamical properties. Generally speaking, for these presented chaotic systems, the Lyapunov exponent spectrums vary gradually and rang from stable equilibrium points, periodic orbits to chaotic oscillations with the changing of system parameters.

[1]Corresponding author.

As a basic and striking theory in chaotic dynamics, topological horseshoe with symbolic dynamics provides a powerful tool in rigorous studies of chaos in dynamical systems. Up till now, remarkable theoretical progress has been made in seeking sufficient conditions for the existence of horseshoes. Kennedy introduced an important chaos lemma which proposed a topological horseshoe theory in continuous map [8, 9]. Yang obtained another concernful criteria to find the topological horseshoe in non-continuous map [10, 11], which have been applied successfully to some practical dynamical systems to present computer-assisted verification of chaos [12–15]. Recently, Li introduced a new method for finding horseshoes in chaotic systems by using several simple results on topological horseshoes [16]. However, it is still a challenge for researchers to seek a topological horseshoe in practical chaotic systems.

This paper proposes a new 3D chaotic system based on the construction pattern of Chen, Liu and Qi chaotic systems. Some basic dynamical characters of the presented chaotic system, such as phase portraits, equilibrium points, bifurcation diagram and Lyapunov exponents are investigated. It's found that with the variation of parameters a, b and c, the novel system can occur period doubling bifurcations. Of particular interest is that the Lyapunov exponent spectrum keeps invariable when the product term parameter e changes. When parameter e increases gradually, the amplitude of the signals x_1, x_2 varies by the power function with a minus half index, but the third one keeps its amplitude in the same range. So we can control the signal amplitude artificially by adjusting e, but the dynamical system is always chaotic. Therefore, it can be concluded that this chaotic system has a more complicated dynamics. Finally, based on the topological horseshoe theory [16], we carefully pick a suitable cross-section with respect to the attractor, and find a topological horseshoe of the corresponding first-returned Poincaré map, thus giving a rigorous confirmation of the chaos existed in this dynamical system.

2 The proposed 3D chaotic system

In the light of construction pattern of Chen, Liu and Qi chaotic systems, a new 3D chaotic system is proposed from Lorenz chaotic system:

$$\begin{cases} \dot{x}_1 = a(x_2 - x_1) + x_2x_3, \\ \dot{x}_2 = (c - a)x_1 - x_1x_3 + cx_2, \\ \dot{x}_3 = ex_2^2 - bx_3, \end{cases} \tag{1}$$

where x_1, x_2, x_3 are the state variables, a, b, c, e are the positive parameters.

2.1 Equilibria and analysis of stability

In order to obtain the equilibria of system (1), let's suppose

$$x_* = \sqrt{\frac{b[(c-2a) + (c^2+4ac)^{0.5}]}{2e}}, \quad y_* = \sqrt{\frac{b[(c-2a) - (c^2+4ac)^{0.5}]}{2e}}.$$

Then, if $2c - a \geqslant 0$, we get three equilibria of system (1):

$$P_0(0,0,0), \quad P_1\left(x_* + \frac{ex_*^3}{ab}, x_*, \frac{ex_*^2}{b}\right), \quad P_2\left(-x_* - \frac{ex_*^3}{ab}, -x_*, \frac{ex_*^2}{b}\right)$$

and if $2c - a < 0$, there are five equilibria in system (1):

$$Q_0(0,0,0), \quad Q_1\left(x_* + \frac{ex_*^3}{ab}, x_*, \frac{ex_*^2}{b}\right), \quad Q_2\left(-x_* - \frac{ex_*^3}{ab}, -x_*, \frac{ex_*^2}{b}\right),$$
$$Q_3\left(y_* + \frac{ey_*^3}{ab}, y_*, \frac{ey_*^2}{b}\right), \quad Q_4\left(-y_* - \frac{ey_*^3}{ab}, -y_*, \frac{ey_*^2}{b}\right).$$

Linearizing system (1) at any equilibrium (x_{10}, x_{20}, x_{30}), it yields the corresponding Jacobian matrix

$$J = \begin{bmatrix} -a & a + x_{30} & x_{20} \\ c - a - x_{30} & c & -x_{10} \\ 0 & 2ex_{20} & -b \end{bmatrix}.$$

The characteristic equation is obtained as follows:

$$f(\lambda) = \lambda^3 + C_2\lambda^2 + C_1\lambda + C_0, \tag{2}$$

where

$$\begin{aligned} C_0 &= -2abc + a^2b - 2e(c - a + x_{30})x_{20}^2 - (c - 2a)bx_{30} + bx_{30}^2 + 2aex_{10}x_{20}, \\ C_1 &= -2ac + ab - bc + a^2 + (2a - c)x_{30} + x_{30}^2 + 2ex_{10}x_{20}, \\ C_2 &= a + b - c. \end{aligned} \tag{3}$$

According to the Routh–Hurwitz criterion, only when $C_2 > 0$, $C_1 > 0$, $C_0 > 0$ and $C_2C_1 - C_0 > 0$, the real parts of all the roots are negative. Thus, there are three unstable equilibria in system (1) when $a = 40$, $b = 5$, $c = 30$, $e = 3$.

2.2 Chaotic phase portraits

When $a = 40$, $b = 5$, $c = 30$, $e = 3$, system (1) is chaotic with the Lyapunov exponents $L_1 = 3.88$, $L_2 = 0.00$, $L_3 = -25.52$. The phase portraits are depicted in Fig. 1. It appears from Fig. 1 that the novel attractor resembles Chen attractor, however, it possesses some interesting characters such as invariable Lyapunov exponent spectrum and controllable amplitude.

2.3 Topological equivalence

Let

$$\dot{x} = g(x) \tag{4}$$

denote the Lorenz (Chen, Liu or Qi) system. And the proposed system (1) is described by

$$\dot{y} = f(y). \tag{5}$$

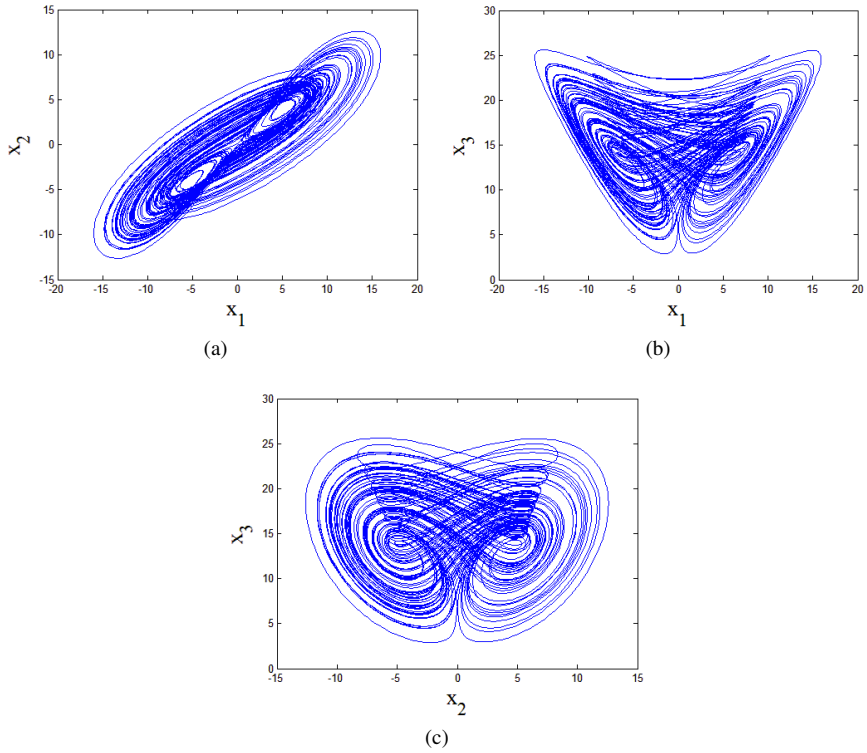

Fig. 1. (a) $x_1 - x_2$ phase portrait; (b) $x_1 - x_3$ phase portrait; (c) $x_2 - x_3$ phase portrait.

Definition 1. (See [17].) If systems (4) and (5) are said to be topological equivalent, then there would exist a diffeomorphism $y = T(x)$, such that

$$g(x) = J^{-1}(x) f\big(T(x)\big),$$

where $J(x) = \mathrm{d}T(x)/\mathrm{d}x$ is the Jacobian matrix of T at the point x.

Let x_0 and $y_0 = T(x_0)$ be the corresponding equilibria of $g(x)$ and $f(x)$, $A(x_0)$ and $B(y_0)$ denote the Jacobians of $g(x)$ and $f(x)$, respectively. If (4) and (5) are topological equivalent, then $A(x_0)$ and $B(y_0)$ are similar, i.e., their characteristic polynomials and eigenvalues should coincide.

Based on the concept and techniques of the equilibrium and resultant eigenvalue, we know that parameter e does not contribute to the eigenvalues of system (1) (see Section 3.3 for concrete analysis), and it is easy to actually verify that the system (5) with any parameter set is not smoothly equivalent to system (4). Therefore, systems (4) and (5) are not topological equivalent, although both have similar attractors.

3 Complex dynamics of novel 3D system by varying each parameter

This system has been found to exhibit complex dynamical behaviors by varying each parameter in a wide range, which is expatiated as below.

3.1 Dynamics of novel system by varying parameters a, b, c

Let a, b, c vary in some region, respectively, but the values of other parameters are set as in Section 2.2. The corresponding bifurcation diagrams are shown in Fig. 2. It's known from Fig. 2, that system (1) has a rich dynamical behavior, ranging from equilibrium points, periodic orbits to chaos, depending on the parameter values.

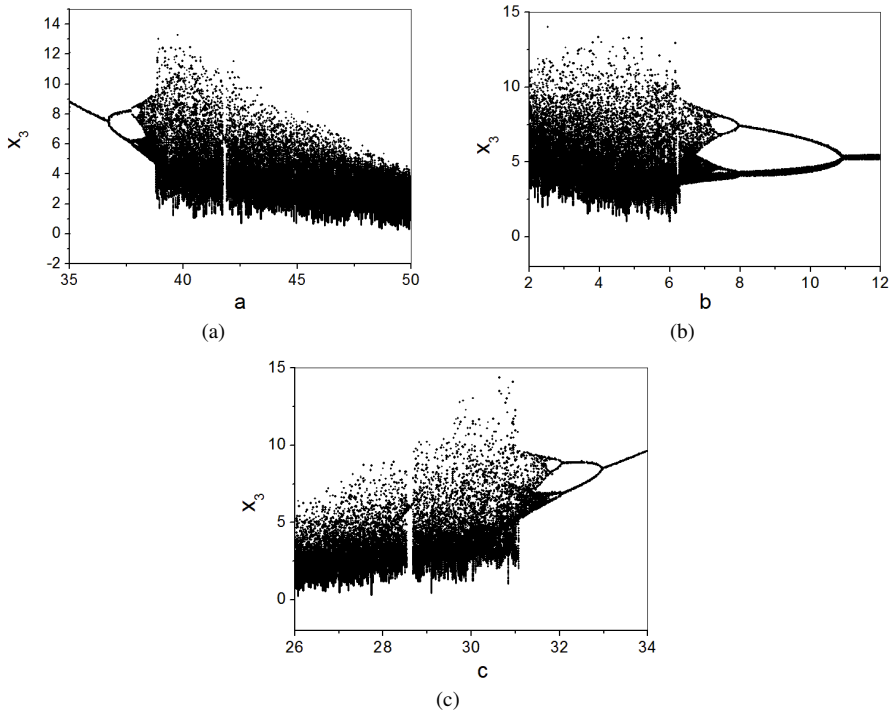

(a) (b) (c)

Fig. 2. Bifurcation diagrams of system (1) versus: (a) parameter a; (b) parameter b; (c) parameter c.

3.2 Dynamics of novel system by varying parameter e

Now, let $a = 40$, $b = 5$, $c = 30$, while e vary in the region $[0, 10]$. The corresponding bifurcation diagram and Lyapunov exponent spectrum are depicted in Fig. 3.

It is notable from Fig. 3 that, when parameter e changes from 0 to 10 gradually, the Lyapunov exponent spectrums keep invariable, and the system is always chaotic.

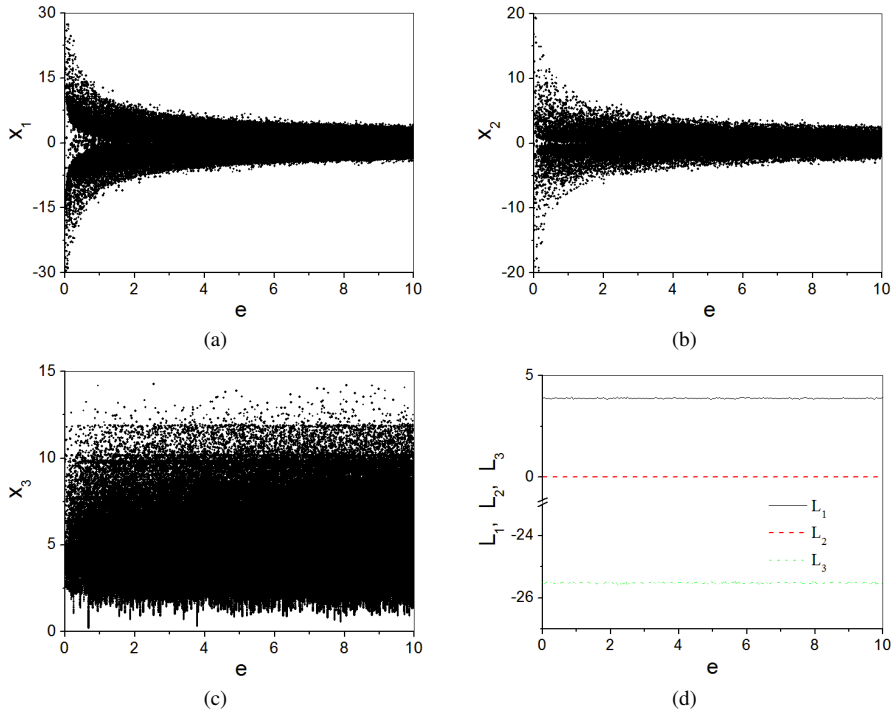

Fig. 3. (a), (b) and (c) bifurcation diagram versus e; (d) Lyapunov exponent spectrum versus e.

Another interesting phenomenon is that, with the increasing of e, the signal amplitude adjusts in certain pattern. Speaking concretely, with the increasing of e, the amplitude of x_1, x_2 decreases nonlinearly, but the amplitude of x_3 keeps in the same range.

3.3 Analysis of constant Lyapunov exponent spectrum

As argued above, the Lyapunov exponent spectrum keeps invariable with the varying of e. In fact, when putting the equilibrium in the coefficient expression (3), we can eliminate the influence of e. For example, when inserting equilibrium P_0 into (3), we obtain

$$C_0 = -2abc + a^2 b, \quad C_1 = -2ac + ab - bc + a^2, \quad C_2 = a + b - c$$

and when substituting equilibrium P_1 or P_2 into (3), we get

$$\begin{aligned} C_0 &= -2abc + a^2 b - \frac{b(3c - 6a)}{2} B_0 + \frac{5b}{4} B_0^2, \\ C_1 &= -2ac + ab - bc + a^2 + \frac{(2a + 2b - c)}{2} B_0 + \frac{(a + 2b)}{4a} B_0^2, \\ C_2 &= a + b - c, \end{aligned}$$

where $B_0 = (c-2a)+(c^2+4ac)^{0.5}$. Therefore, the eigenvalues relating to characteristic equation (2) are irrespective parameter e, and when parameter e varies, the Lyapunov exponent spectrum remains constant.

3.4 Analysis of amplitude control

It's known from the forementioned analysis, with the increasing of e, the signal amplitudes vary according to some criteria.

Theorem 1. *The coefficient e of the square term x_2^2 is a local parameter of nonlinear amplitude adjuster, and with the increasing of e, the amplitude of x_1, x_2 changes by the power function with an index of $-1/2$, but the third one keeps its amplitude in the same range.*

Proof. Let $x_1 = k^{0.5}x_1^*$, $x_2 = k^{0.5}x_2^*$, $x_3 = x_3^*$ $(k > 0)$, then system (1) can be transformed to

$$\begin{cases} \dot{x}_1^* = a(x_2^* - x_1^*) + x_2^* x_3^*, \\ \dot{x}_2^* = (c-a)x_1^* - x_1^* x_3^* + cx_2^*, \\ \dot{x}_3^* = ekx_2^{*2} - bx_3^*, \end{cases}$$

therefore, the amplitude adjuster of signals x_1, x_2, x_3 correspond to the variety of parameter e, and when e increases successively, the amplitude of x_1, x_2 changes by the power function with an index of $-1/2$, but the amplitude of x_3 keeps in the same range.

As a numerical explanation, we consider the influence of parameter e on the amplitude of x_1, x_2, x_3, as described in Fig. 4. Clearly, when $e = 2$, the amplitude of signals x_1, x_2 is two times as large as the one with $e = 4$; and the amplitude of x_3 is same as the case with $e = 4$. □

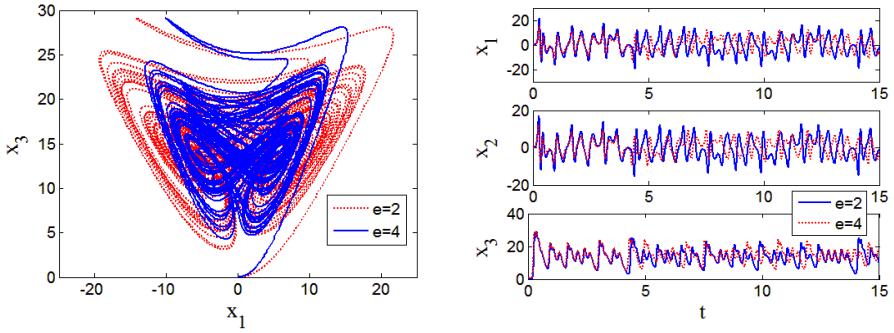

(a) (b)

Fig. 4. Phase portrait and time series of system (1) with different e: (a) phase portrait; (b) time series.

4 Review of topological horseshoe theorem

Before introducing the results on topological horseshoe, we should first recall the concept of m-shift map.

Let $S_m = \{1, 2, \ldots, m\}$ be the set of non-negative integer from 1 to m. And let space $\sum_m$ be the collection of all one-sided infinite sequences with the elements S_m , i.e., each element s of $\sum_m$ is of the following form:

$$s = \{s_1, s_2, \ldots, s_m, \ldots\}, \quad s_i \in S_m.$$

Now let's consider another sequence $\tilde{s}(\tilde{s} \in S_m)$. Then the distance between s and $\tilde{s}$ can be defined as follows:

$$d(s, \tilde{s}) = \sum_{i=1}^{\infty} \frac{|s_i - \tilde{s}|}{2^i(|s_i - \tilde{s}| + 1)}.$$

With the distance defined as above equation, $\sum_m$ is a metric space.

A m-shift map $\sigma : \sum_m \to \sum_m$ is defined as

$$\sigma(s_i) = s_{i+1}.$$

As a dynamical system defined on $\sum_m$, the shift map σ has:

(a) a countable infinity of periodic orbits consisting of orbits of all periods;
(b) an uncountable infinity of nonperiodic orbits;
(c) a dense orbit.

A consequence of these three properties is that the dynamics generated by the shift map σ displays sensitive dependence on the initial conditions, therefore is chaotic.

Let S be a separable metric space and $E \subset S$ is a compact subset, and there exist m mutually disjoint compact subsets $E_1, E_2, \ldots, E_m$ of E. $f : E \to S$ is a map and $f \mid E_i$, the restriction of f to each E_i, is continuous.

Definition 2. (See [18].) For each $1 \leqslant i \leqslant m$, let $E_i^1, E_i^2 \subset E_i$ be two fixed disjoint compact subsets. If $\gamma \cap E_i^1$ and $\gamma \cap E_i^2$ are nonempty and compact, we say a connected subset γ of E_i connect E_i^1 and E_i^2, and we denote this by $E_i^1 \overset{\gamma}{\leftrightarrow} E_i^2$

Definition 3. (See [18].) Let γ be a connected subset of E_i, if there exists a connected subset $\gamma_i \subset \gamma$ such that $f(\gamma_i) \subset E_i$, and $f(\gamma_i) \cap E_i^1$ and $f(\gamma_i) \cap E_i^2$ are nonempty, we call $f(\gamma)$ is suitably across E_i with respect to E_i^1 and E_i^2. In this case, we denote it by $f(\gamma) \mapsto E_i$.

Definition 4. Let S and $\sum_m$ be two topological spaces, $f : S \to S$ and $g : \sum_m \to \sum_m$ are continuous functions. If there exists a continuous surjection $h : \sum_m \to S$ such that $foh = hog$, we say that f is topologically semiconjugate to g .

Lemma 1. (*See* [16].) *Let m be a positive integer, if $f^p(E_i) \mapsto E_i$, then $f^{mp}(E_i) \mapsto E_i$.*

Theorem 2. (*See* [16].) *If $f^p(E_1) \mapsto E_1$, $f^p(E_1) \mapsto E_2$ and $f^q(E_2) \mapsto E_1$, then a compact invariant set $\Lambda \subset E$ will be found, such that $f^{2p+p} \mid \Lambda$ is semiconjugate to 2-shift dynamics, and we have* $\mathrm{ent}(f) \geqslant (q + 1/2p) \log 2$ *, here* $\mathrm{ent}(f)$ *denotes the topological entropy of f.*

5 Topological horseshoe in the novel chaotic system

It is no easy job to seek topological horseshoes in a dynamical system, especially to select a suitable polygon in the cross-section. In this section we will search the horseshoe existed in system (1) by using the topological horseshoe theorem in Section 4.

We consider the plane $\Gamma = \{(x_1, x_2, x_3) \in R^3\colon\ x_2 = 0\}$, and the parameters of system (1) is selected as $a = 40$, $b = 5$, $c = 30$, $e = 3$. As shown in Fig. 5, the four vertices of the corresponding quadrilateral P on this plane is selected as $(-8, 0, 5)$, $(1, 0, 5)$, $(1, 0, 25)$, $(-8, 0, 25)$.

First, in the cross-section P, after a great deal of computer simulations, we select a quadrilateral E_1 with the vertices $A_1(-1.714, 0.0, 12.077)$, $B_1(-1.545, 0.0, 12.714)$, $C_1(-1.102, 0.0, 11.423)$, $D_1(-1.241, 0.0, 10.786)$. The Poincaré map $H : E_1 \to P$ is defined as below: for each point $x \in E_1$, $H(x)$ is the first return intersection point with P under the flow with initial condition x.

Precisely, let $d1r$ and $d1l$ denote the right and left sides of E_1, respectively. Numerical simulations show that, under the map H, the image $H(x)(x \in E_1)$ lies wholly across the quadrilateral E_1, and $H(d1r)$ lies on the left side of A_1B_1, $H(d1l)$ lies on the right side of C_1D_1. For the details, see Fig. 6.

Then, we will take a quadrilateral E_2 such that $H(E_2) \mapsto E_1$ and $H(E_1) \mapsto E_2$. By many trial-and-error numerical simulations, we pick the four vertexes of E_2 as $A_2(-2.380, 0.0, 14.071)$, $B_2(-2.317, 0.0, 14.283)$, $C_2(-2.089, 0.0, 13.728)$, $D_2(-2.152, 0.0, 13.499)$, respectively.

Similarly, we suppose $d2r$ and $d2l$ denote the right and left sides of E_2, respectively. The first return Poincaré map $H(E_2)$ is described as Fig. 7. Obviously, $H(d2r)$ lies on the right side of C_1D_1, $H(d2l)$ lies on the left side of A_1B_1, therefore, the image $H(x)(x \in E_2)$ is wholly across the quadrangle E_1.

Thus, according to Theorem 2, there exists a compact invariant set $\Lambda \subset E$, such that $H^3 \mid \Lambda$ is semiconjugate to 2-shift dynamics, and $\mathrm{ent}(H) \geqslant 1.5 \log 2 > 0$. Thereby it indicates that the attractor depicted in Fig. 5 is chaotic.

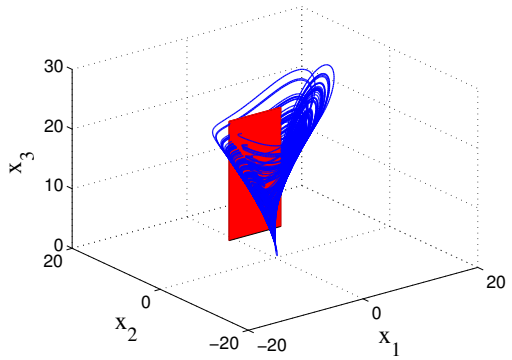

Fig. 5. Poincaré cross-section of system (1).

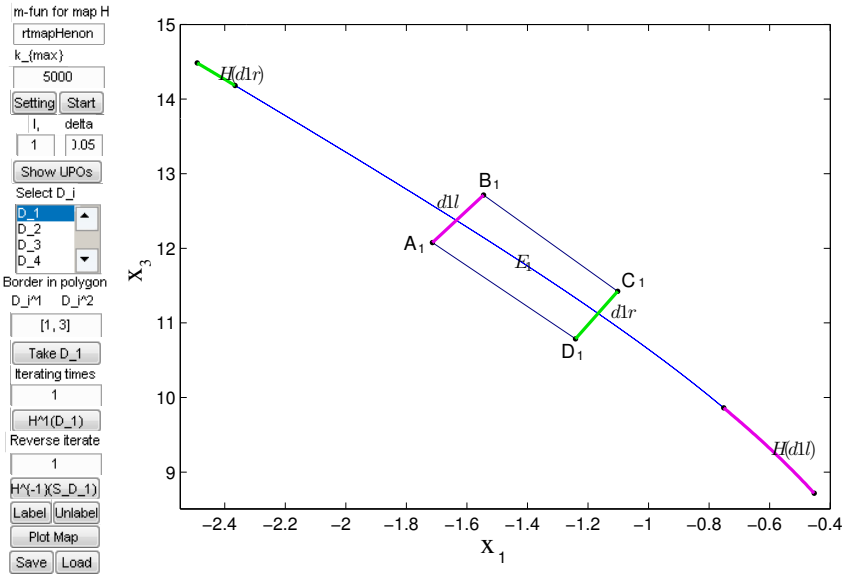

Fig. 6. The subset E_1 and its image.

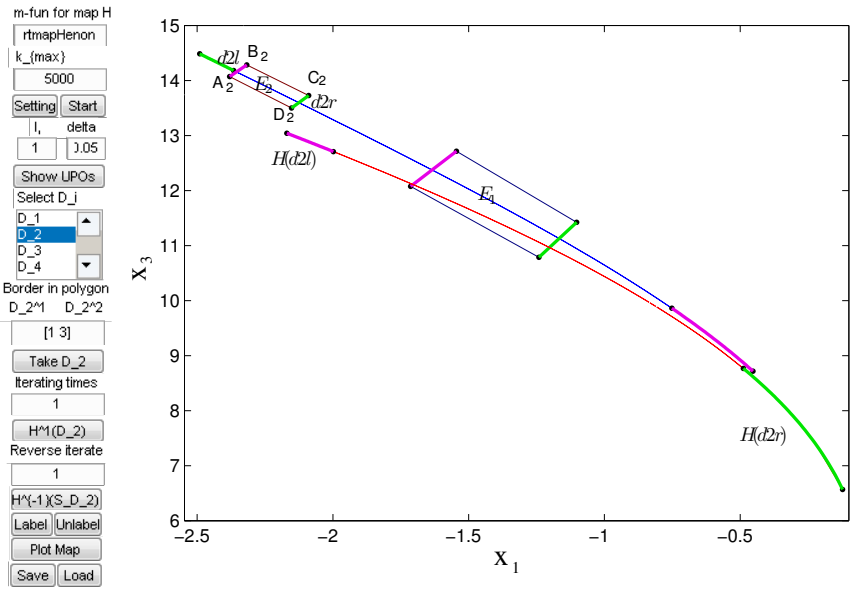

Fig. 7. The subset E_2 and its image.

6 Conclusion

In this paper, a new chaotic system has been proposed from Lorenz system. Some basic properties of the presented chaotic system have been studied in terms of phase portraits, equilibrium points, bifurcation diagram and Lyapunov exponent spectrum. Careful investigation reveals that with the variation of parameters a, b and c, a period-doubling sequence of bifurcations leads to chaos. An interesting phenomenon is that the Lyapunov exponent keeps constant while parameter e varies. And with the increasing of parameter e, the amplitude of the signals x_1, x_2 change by the power function with an index of $-1/2$, but the third one keeps in the same range. Finally, the horseshoe chaos in this system is investigated based on the topological horseshoe theory.

References

1. E.N. Lorenz, Deterministic non-periodic flow, *J. Atmos. Sci.*, **20**, pp. 130–141, 1963.

2. X.Y. Wang, M.J. Wang, A hyperchaos generated from Lorenz system, *Physica A*, **387**, pp. 3751–3758, 2008.

3. C. Ma, X.Y. Wang, Bridge between the hyperchaotic Lorenz system and the hyperchaotic Chen system, *Int. J. Mod. Phys. B*, **25**, pp. 711–721, 2011.

4. G.R. Chen, T. Ueta, Yet another chaotic attractor, *Int. J. Bifurcation Chaos Appl. Sci. Eng.*, **9**, pp. 1465–1466, 1999.

5. C.X Liu, T. Liu, L. Liu, K. Liu, A new chaotic attractor, *Chaos Solitons Fractals*, **22**, pp. 1031–1038, 2004.

6. G.Y. Qi, G.R. Chen, M. Wyk, A four-wing chaotic attractor generated from a new 3-D quadratic autonomous system, *Chaos Solitons Fractals*, **38**, pp. 705–721, 2008.

7. J.H. Lü, G.R. Chen, A new chaotic attractor coined, *Int. J. Bifurcation Chaos Appl. Sci. Eng.*, **12**, pp. 659–661, 2002.

8. J. Kennedy, J.A. York, Topological horseshoes, *Trans. Am. Math. Soc.*, **353**, pp. 2513–2530, 2001.

9. J. Kennedy, S. Kocak, J.A. York, A chaos lemma, *Am. Math. Mon.*, **108**, pp. 411–423, 2001.

10. X.S. Yang, Y. Tang, Horseshoes in piecewise continuous maps, *Chaos Solitons Fractals*, **19**, pp. 841–845, 2004.

11. X.S. Yang, Topological horseshoes and computer assisted verification of chaotic dynamics, *Int. J. Bifurcation Chaos Appl. Sci. Eng.*, **19**, pp. 1127–1145, 2009.

12. W.Z. Huang, Y. Huang, Chaos, bifurcation and robustness of a class of Hopfield neural networks, *Int. J. Bifurcation Chaos Appl. Sci. Eng.*, **21**, pp. 885–895, 2011.

13. Q. Yuan, Q.D. Li, X.S. Yang, Horseshoe chaos in a class of simple Hopfield neural networks, *Chaos Solitons Fractals*, **39**, pp. 1522–1529, 2009.

14. Q.D. Li, X.S. Yang, S. Chen, Hyperchaos in a spacecraft power system, *Int. J. Bifurcation Chaos Appl. Sci. Eng.*, **21**, pp. 1719–1726, 2011.

15. C. Ma, X.Y. Wang, Hopf bifurcation and topological horseshoe of a novel finance chaotic system, *Commun. Nonlinear Sci. Numer. Simul.*, **17**, pp. 721–730, 2012.

16. Q.D. Li, X.S. Yang, A simple method for finding topological horseshoes, *Int. J. Bifurcation Chaos Appl. Sci. Eng.*, **20**, pp. 467–478, 2010.

17. Y.A. Kuznetsov, *Elements of Applied Bifurcation Theory*, 2nd edition, Springer, New York, 1998.

18. X.S. Yang, Topological horseshoes in continuous maps, *Chaos Solitons Fractals*, **33**, pp. 225–233, 2007.